iScience

CellPress
OPEN ACCESS

Article

Rickettsial pathogen inhibits tick cell death through tryptophan metabolite mediated activation of p38 MAP kinase

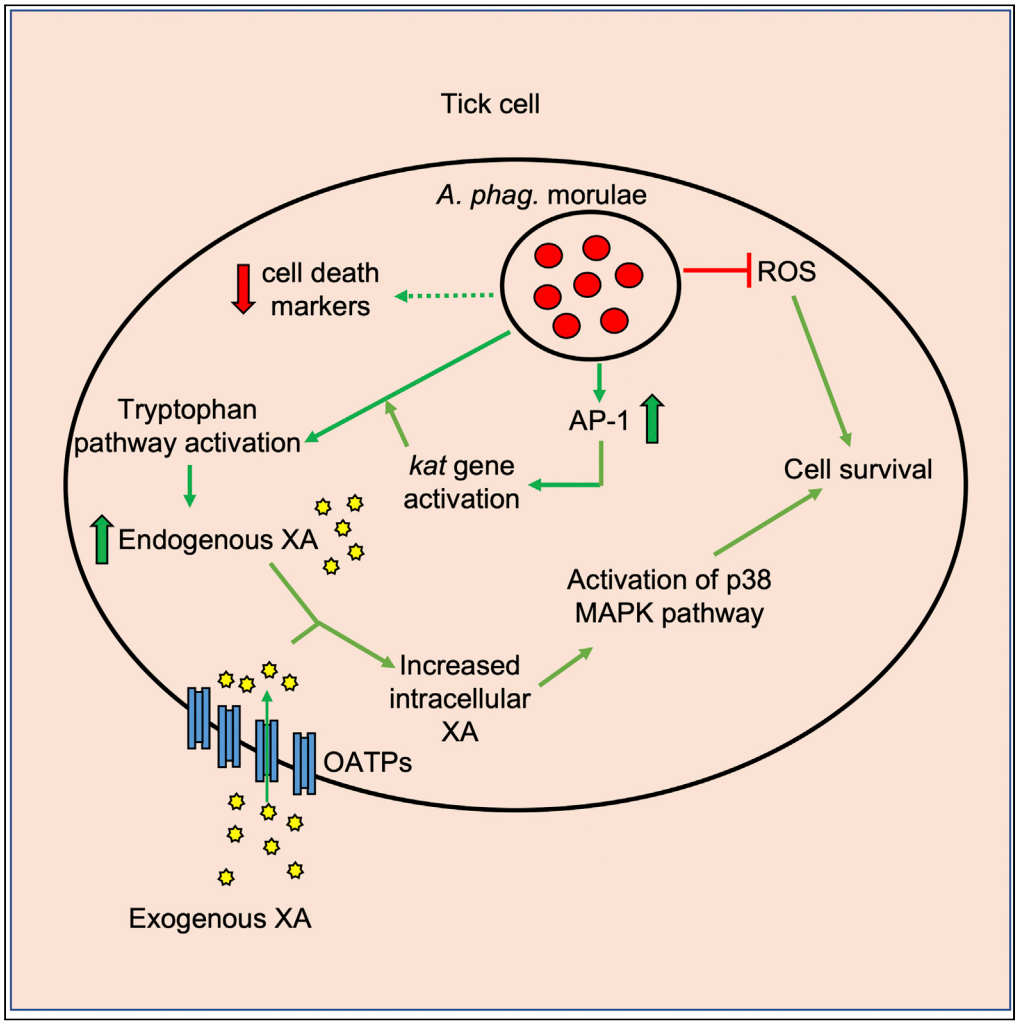

Prachi Namjoshi, Mustapha Dahmani, Hameeda Sultana, Girish Neelakanta

gneelaka@utk.edu

Highlights

Anaplasma phagocytophilum infection inhibits tick cell death

Tryptophan metabolite, xanthurenic acid, activates p38 MAPK

Tick tryptophan and p38 MAPK pathways are critical for *A. phagocytophilum* survival

Namjoshi et al., iScience 26, 105730
January 20, 2023 © 2022 The Author(s).
https://doi.org/10.1016/j.isci.2022.105730

iScience

CellPress
OPEN ACCESS

Article

Rickettsial pathogen inhibits tick cell death through tryptophan metabolite mediated activation of p38 MAP kinase

Prachi Namjoshi,[1] Mustapha Dahmani,[2] Hameeda Sultana,[1] and Girish Neelakanta[1,3,*]

SUMMARY

***Anaplasma phagocytophilum* modulates various cell signaling pathways in mammalian cells for its survival. In this study, we report that *A. phagocytophilum* modulates tick tryptophan pathway to activate arthropod p38 MAP kinase for the survival of both this bacterium and its vector host. Increased level of tryptophan metabolite, xanthurenic acid (XA), was evident in *A. phagocytophilum*-infected ticks and tick cells. Lower levels of cell death markers and increased levels of total and phosphorylated p38 MAPK was noted in *A. phagocytophilum*-infected ticks and tick cells. Treatment with XA increased phosphorylated p38 MAPK levels and reduced cell death in *A. phagocytophilum*-infected tick cells. Furthermore, treatment with p38 MAPK inhibitor affected bacterial replication, decreased phosphorylated p38 MAPK levels and increased tick cell death. However, XA reversed these effects. Taken together, we provide evidence that rickettsial pathogen modulates arthropod tryptophan and p38 MAPK pathways to inhibit cell death for its survival in ticks.**

INTRODUCTION

Ticks are arthropod vectors that transmit various pathogens to mammalian hosts.[1,2] *Ixodes scapularis*, a black-legged tick, is a primary vector in the transmission of zoonotic rickettsial pathogen, *A. phagocytophilum*, to various hosts like humans, horses, cattle, deer, and dogs.[3–5] These ticks have four developmental stages in their life cycle that includes eggs, larvae, nymph, and adult stage.[6] When immature *I. scapularis* takes a blood meal from an *A. phagocytophilum*-infected reservoir host, this bacterium enters tick through a blood meal and is then transstadially maintained in different developmental stages of these ticks.[7] Humans or other vertebrate animals could get infected with this bacterium on bite by an *A. phagocytophilum*-infected tick.[4,7]

A. phagocytophilum is an obligate intracellular gram-negative bacterium that causes human granulocytic anaplasmosis (HGA).[8] In humans, *A. phagocytophilum* infects, resides, and replicates in neutrophils.[9,10] Soon after entry into the host cells, *A. phagocytophilum* resides and multiplies within a host-derived vacuole.[4] The host-derived vacuoles are noted to be intact throughout *A. phagocytophilum* infection cycle and enlarges as the bacterial number increases.[4] The expansion of host-derived vacuoles was reported to be likely because of acquisition of membranes from autophagosomes, trans-Golgi vesicles and ER-derived vesicles.[11–13] In addition, *A. phagocytophilum* is known to utilize various nutritional virulence strategies, including hijacking the epigenetic machinery of the host cells,[14] acquisition of host cholesterol,[15] modulation of vesicular trafficking to persist in the vacuoles,[4] evasion of autophagy[11] and delayed apoptosis.[4] Several studies, including our own, have reported that *A. phagocytophilum* also modulates various signaling cascades to survive in ticks.[1,16–29]

On bacterial, viral and parasitic infections, host cells induce cell death to eventually result in the decline of the infecting pathogen.[30] However, pathogens have developed unique strategies to inhibit host cell death for their survival and replication. Apoptosis is a well characterized type of a programmed cell death mechanism.[30] Several pathogens, including *A. phagocytophilum*, have developed strategies to inhibit apoptosis of host cells.[30,31] In mammalian cells, *A. phagocytophilum* inhibits activation of apoptotic caspase cascade, increases expression of anti-apoptotic genes, and transfer *Anaplasma* translocated substrate-1 (Ats-1) to interfere with apoptosis induction.[11,31] In addition, p38 mitogen-activated protein kinase (p38 MAPK)

[1]Department of Biomedical and Diagnostic Sciences, College of Veterinary Medicine, University of Tennessee, Knoxville, TN 37996, USA

[2]Department of Veterinary Medicine, University of Maryland-College Park, College Park, MD, USA

[3]Lead contact

*Correspondence: gneelaka@utk.edu

https://doi.org/10.1016/j.isci.2022.105730

This is an open access article under the CC BY-NC-ND license (http://creativecommons.org/licenses/by-nc-nd/4.0/).

signal transduction pathway has been reported to be involved in the delayed apoptosis in *A. phagocytophilum*-infected human neutrophils.[32] In the vector host, *A. phagocytophilum* inhibits apoptosis in *I. scapularis* cell line, ISE6, by downregulation of mitochondrial porin.[23] In tick salivary glands, *A. phagocytophilum* inhibits the intrinsic apoptosis pathway whereas in guts this bacterium inhibits apoptosis through Janus kinase/signal transducers and activators of transcription (JAK/STAT) pathway.[26] These studies highlight that *A. phagocytophilum* has developed strategies to survive in both mammalian and vector host cells by inhibiting apoptosis.

In our previous work, we reported that *A. phagocytophilum* modulates organic anion transporting polypeptide (OATP) and tryptophan pathway to survive in *I. scapularis* ticks.[17] Xanthurenic Acid (XA), a metabolite from the tryptophan pathway, is synthesized from 3-hydroxy-L-kynurenine through kynurenine amino transferase (KAT) activity. RNAi-mediated knockdown of *isoatp4056* or *kat* expression, alone or in combination, significantly affected *A. phagocytophilum* growth in ticks and tick cells.[17] Exogenous addition of XA resulted in increased *A. phagocytophilum* burden in tick cells and in tick salivary glands.[17] In addition, we noted that *A. phagocytophilum* modulates tryptophan pathway to prevent build-up of reactive oxygen species (ROS) levels in tick cells.[18] Studies have reported that XA induces development of malarial parasite *Plasmodium falciparum* in mosquitoes.[33,34] A recent study has reported an antioxidant role for XA in *Aedes aegypti* mosquitoes.[35] In the same study, it has been reported that lack of XA promoted cell death in the mosquito midgut epithelium.[35] The molecular mechanism on how lack of XA could lead to cell death is not known. Moreover, there is no evidence that suggests whether pathogens modulate XA to prevent their host cell death. In this study, we provide evidence that *A. phagocytophilum* not only induces XA levels in ticks but also concurrently activates p38 MAPK pathway to prevent cell death in its vector host.

RESULTS

Exogenous treatment with tryptophan metabolite, XA, increases survival of *A. phagocytophilum*-infected tick cells

Previous studies from our laboratory have reported that *A. phagocytophilum* modulates tryptophan pathway for its survival in ticks.[17–19] Exogenously added tryptophan metabolite, XA, at 100 μM increased *A. phagocytophilum* burden in both ticks and tick cells.[17–19] To test whether XA has any effect on tick cell survival, we performed live/dead assay. In the live/dead assay, live cells stain green and dead cells stain red. Based on this assay, we found that XA-treated uninfected or *A. phagocytophilum*-infected tick cells exhibited significantly reduced cell death on days 1, 3 and 6 after infection as compared to the respective mock-treated controls (Figure 1A). The cell death observed on days 1, 3 and 6 is normal for the cell line used in this study. Quantification of fluorescence intensity of dead cells in mock or XA-treated uninfected or *A. phagocytophilum*-infected cells further confirmed these microscopic observations (Figure 1B). We noted significantly ($p < 0.05$) smaller number of dead cells in XA-treated uninfected or *A. phagocytophilum*-infected tick cells compared to the respective mock controls (Figure 1B). These results show that exogenously added XA facilitates increased survival of tick cells.

Sequence analysis of potential cell death markers in *I. scapularis*

The observation of reduced tick cell death in the presence of XA (Figure 1) promoted us to investigate tick cell death markers. Studies have reported that Phospholipase D3 (PLD3), Senescence marker protein 30 (SMP30), Syntaxin and Vacuolar protein sorting 26B (VPS26B) proteins are involved in cell death process.[36–39] *I. scapularis* ticks encodes all these genes in their genome (Table S1). Percent identity of *I. scapularis* SMP30 (Figure S1A), Syntaxin (Figure S1B), PLD3 (Figure S1C), and VPS26B (Figure S1D) amino acid sequence with ortholog proteins from *Homo sapiens* (Hs), *Mus musculus* (Mm), *Drosophila melanogaster* (Dm), *Anopheles gambiae* (Ag), *Culex quinquefasciatus* (Cq) and *A. aegypti* (Aa) were determined by CLUSTALW alignment. *I. scapularis* SMP30 amino acid sequence shares 36%, 35%, 33%, 35%, 35% and 33% identity with human, mouse, *D. melanogaster*, *A. gambiae*, *C. quinquefasciatus*, and *A. aegypti* SMP30 orthologs, respectively (Figures S1A and S2A). *I. scapularis* syntaxin amino acid sequence shares 69%, 69%, 73%, 74%, 75% and 75% identity with human, mouse, *D. melanogaster*, *A. gambiae*, *C. quinquefasciatus*, *A. aegypti* syntaxin orthologs, respectively (Figures S1B and S2B). *I. scapularis* PLD3 amino acid sequence shares 41%, 43%, 46% 50%, 48% and 49% identity with human, mouse, *D. melanogaster*, *A. gambiae*, *C. quinquefasciatus*, and *A. aegypti* PLD3 orthologs, respectively (Figures S1C and S2C) and *I. scapularis* VPS26B amino acid sequence shares 80%, 80%, 77%, 80%, 79% and 79% identity with human, mouse, *D. melanogaster*, *A. gambiae*, *C. quinquefasciatus*, *A.aegypti* VPS26B orthologs, respectively (Figures S1D and S2D). Domain analysis of *I. scapularis* syntaxin primary amino acid sequence showed presence of

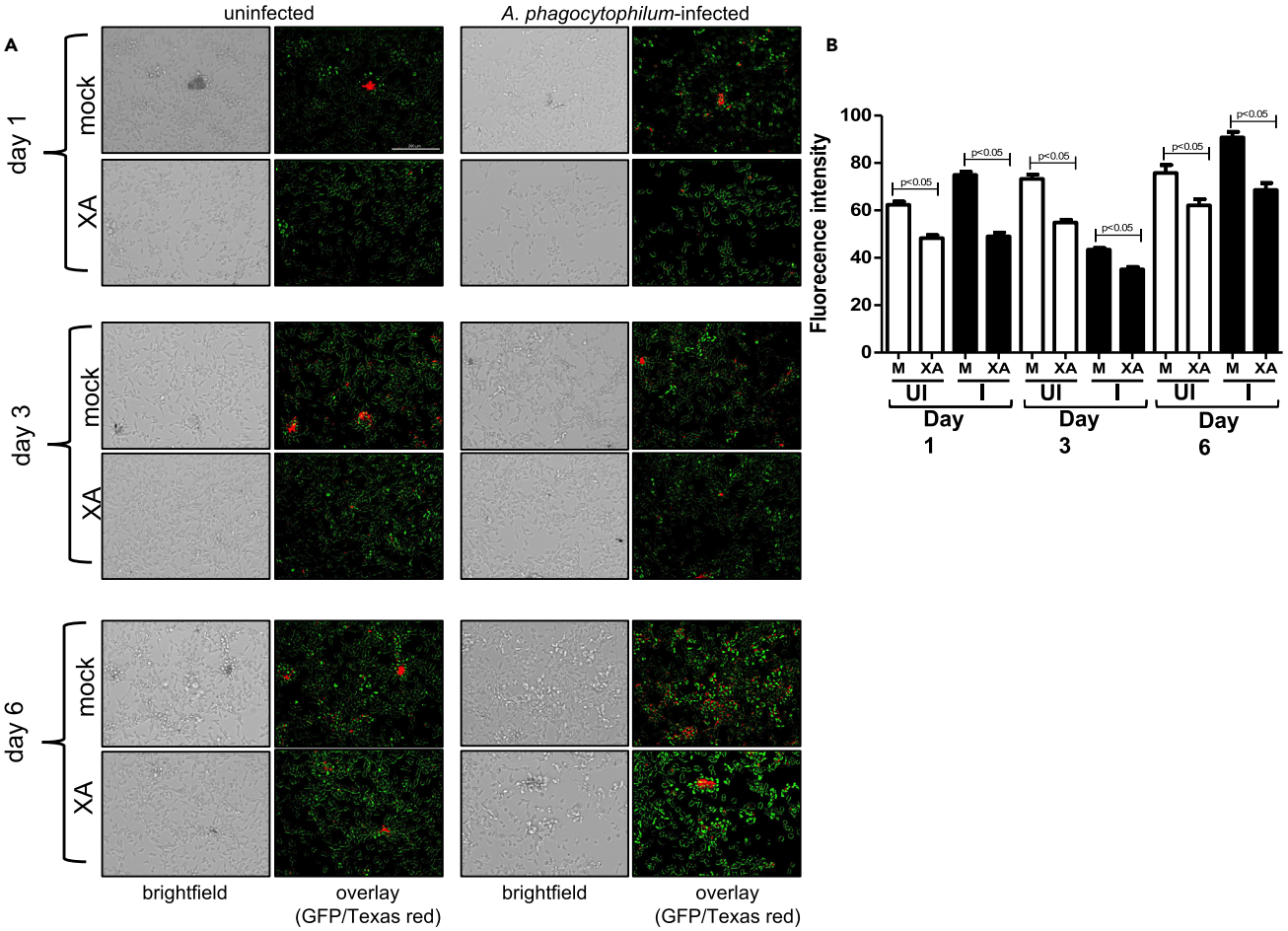

Figure 1. Exogenous treatment with XA inhibits tick cell death

(A) Phase contrast or fluorescent microscopic images showing live (green) and dead (red) uninfected or *A. phagocytophilum*-infected tick cells. Tick cells were treated with either mock or XA and processed for staining using Live/Dead staining kit on days 1, 3 and 6 after treatment, followed by imaging using fluorescent microscope. Scale bar indicates 200 μm.

(B) Quantification of fluorescence intensity measurement of dead cells (red) from Live/dead-assay performed with XA-treated uninfected or *A. phagocytophilum*-infected tick cells. Open and black bars indicate fluorescence intensity measured from uninfected or *A. phagocytophilum* tick cells, respectively. Statistical analysis was performed using Student's *t* test and p value is shown.

transmembrane region domain (279–293 aa) at C-terminus, one SynN domain (29–151aa) and t-SNARE domain (192–259aa) (Figure S1E). Domain analysis of *I. scapularis* PLD3 primary amino acid sequence showed presence of transmembrane region domain (89–111 aa) at N-terminus, two phospholipase D active site (PLDc) motifs (262–289 aa, 480–506 aa) and PLD-like domain (Pfam:PLDc_3) (292–471aa) (Figure S1F). Phylogenetic tree analysis of PLD3 showed *I. scapularis* PLD3 to group into a different clade than rest of the orthologs. (Figure S1G). PLD3 ortholog from *D. melanogaster* forms a clade close to human and mice orthologs. Whereas PLD3 orthologs from mosquitoes form a separate clade (Figure S1G). The sequence analysis of *I. scapularis* Syntaxin, VPS26B and SMP30 revealed that tick proteins form a clade close to *D. melanogaster* and mosquito proteins and human and mice proteins form a different clade (Figure S3). Bioinformatic analysis of post translational modification sites in *I. scapularis* PLD3, SMP30, Syntaxin and VPS26B revealed that these proteins have several N-myristoylation, Protein kinase II phospho, N-glycosylation, cAMP and cGMP and protein kinase C phospho sites (Figure S4).

Expression of *smp30, syntaxin, pld3* and *vps26b* is developmentally regulated

Ticks have four life cycle stages. Therefore, we analyzed whether *smp*30, *syntaxin*, *pld3* and *vps26b* transcripts are expressed in all tick developmental stages (Figure 2). qPCR analysis showed that larvae expressed significantly ($p < 0.05$) higher levels of *smp30* (Figure 2A) and *pld3* (Figure 2C) in comparison to

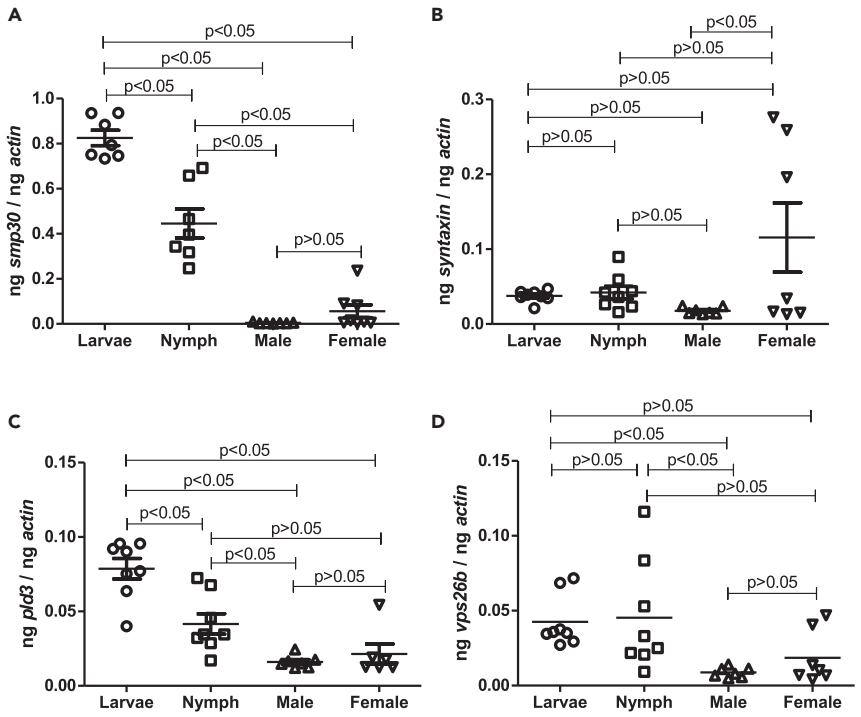

Figure 2. The levels of *smp30, syntaxin, pld3 and vps26b* transcripts at different developmental stages of *I. scapularis*

(A–D) Quantitative PCR (qPCR) analysis showing expression of *smp30* (A), *syntaxin* (B), *pld3* (C), *vps26b* (D) at different tick developmental stages in uninfected unfed ticks. Each data point in nymphs and adult samples represents transcript levels noted in an individual tick. For larval samples, each data point represents transcript levels noted in five pooled larvae. Horizontal lines in the graphs represents mean of the data points. The mRNA levels of these genes are normalized to tick beta-actin mRNA levels. Statistical significance was calculated using ANOVA analysis.

levels noted in nymphs, male and female ticks. Nymphs expressed significantly ($p < 0.05$) higher levels of *smp30* mRNA in comparison to both male and female ticks (Figure 2A). In addition, nymphs expressed significantly higher levels of *pld3* mRNA in comparison to the levels noted in male ticks (Figure 2C). Although no significant ($p > 0.05$) differences in the *pld3* mRNA levels was observed between nymph and female ticks (Figure 2C). No significant ($p > 0.05$) differences in the expression of *syntaxin* mRNA levels were noted between larvae, nymphs, and adult male ticks. However, significant ($p < 0.05$) differences in the expression of *syntaxin* mRNA levels was noted between male and female ticks (Figure 2B). Larvae and nymphs expressed significantly ($p < 0.05$) higher levels of *vps26b* when compared to levels noted in male ticks (Figure 2D). However, no significant ($p > 0.05$) differences in the *vps26b* levels were noted between larvae and nymphs when compared to the levels noted in female ticks (Figure 2D). These datashow variable expression pattern of *smp30*, *syntaxin*, *pld3* and *vps26b* transcript levels at different developmental stages of ticks.

A. phagocytophilum downregulates expression of *smp30, syntaxin and pld3* transcript levels in nymphal ticks and tick cells

We analyzed whether *A. phagocytophilum* modulates expression of cell death markers. mRNA transcript levels of cell death markers were analyzed in uninfected or *A. phagocytophilum*-infected unfed nymphal ticks as well as in uninfected or *A. phagocytophilum*-infected tick cells (Figure 3). qPCR analysis revealed that expression of *smp30* (Figure 3A), *syntaxin* (Figure 3B), *pld3* (Figure 3C) but not of *vps26b* (Figure 3D) were significantly decreased in *A. phagocytophilum*-infected ticks when compared to levels noted in uninfected nymphal ticks. In addition, we noted decreased expression of *smp30* (Figure 3E), *syntaxin* (Figure 3F), *pld3* (Figure 3G) and *vps26b* (Figure 3H) in *A. phagocytophilum*-infected tick cells when compared to expression noted in uninfected controls. As expected, qPCR analysis confirmed presence of *A. phagocytophilum* in only infected ticks and tick cells (Figures S5A and S5B). Immunoblotting analysis further confirmed that PLD3 is three-to 4-fold downregulated in *A. phagocytophilum*-infected ticks in comparison

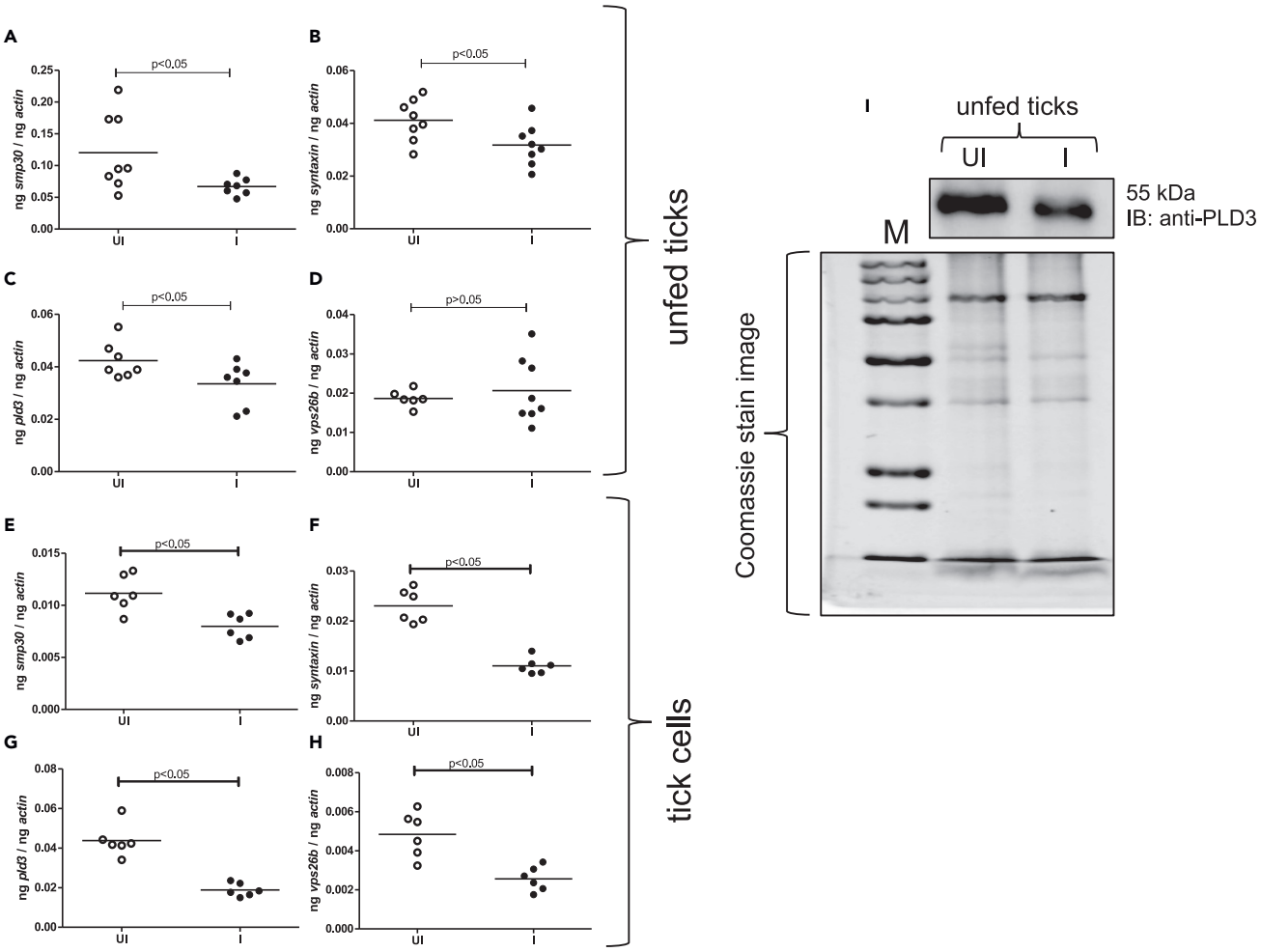

Figure 3. *Anaplasma phagocytophilum* downregulates expression of *smp30, syntaxin and pld3* mRNA levels in unfed *I. scapularis* nymphs and tick cells

(A–I) Quantitative PCR analysis showing expression of *smp30* (A and E), *syntaxin* (B and F), *pld3* (C and G), *vps26b* (D and H) in unfed uninfected or *A. phagocytophilum*-infected ticks (A–D) and uninfected or *A. phagocytophilum*-infected tick cells (E–H) at 48 h p.i. Open circles represent uninfected (UI) and closed circles represent infected (I) ticks or tick cells. In panels (A–D), each circle represents data from samples generated from one tick and in panels (E–H), each circle represents data from tick cell samples generated from one independent culture plate well in a plate. Horizontal lines in the graphs represents mean of the data points. The mRNA levels of these genes were normalized to tick beta-actin mRNA levels. p value from Student's *t* test is shown.

(I) Immunoblotting analysis showing levels of PLD3 in uninfected (UI) or *A. phagocytophilum*-infected (I) unfed nymphal ticks. Coomassie blue stained gel image for total protein profile serves as loading control in the immunoblotting analysis. M indicates Precision Plus protein all blue marker from BioRad, USA.

to the levels noted in uninfected ticks (Figures 3I and S5C, Table S3). These results indicate that expression of cell death marker transcripts is downregulated in *A. phagocytophilum*-infected ticks and tick cells.

A. phagocytophilum increases endogenous levels of tryptophan metabolite XA in nymphal ticks and tick cells

Our previous studies reported that *A. phagocytophilum* upregulates *isoatp4056* and kynurenine amino transferase (*kat*) genes that facilitates bacterial replication in both ticks and tick cells.[17–19] Because we noted that tick cells exhibited increased cell survival (Figures 1A and 1B) and reduced levels of cell death markers in presence of *A. phagocytophilum* infection (Figure 3), we examined if *A. phagocytophilum* influences the endogenous levels of XA in ticks and tick cells (Figure 4). Quantification of endogenous levels of XA was determined by a highly specific colorimetric method which is based on formation of pigment by XA and *N, N*-diethyl-*p*-phenylenediamine (DE-PPD) oxidative coupling.[40] This assay is highly specific for XA determination and do not measure kynurenic acid (KA) (Figure 4A). We noted significantly ($p < 0.05$) increased levels of endogenous XA in unfed *A. phagocytophilum*-infected nymphs when compared to

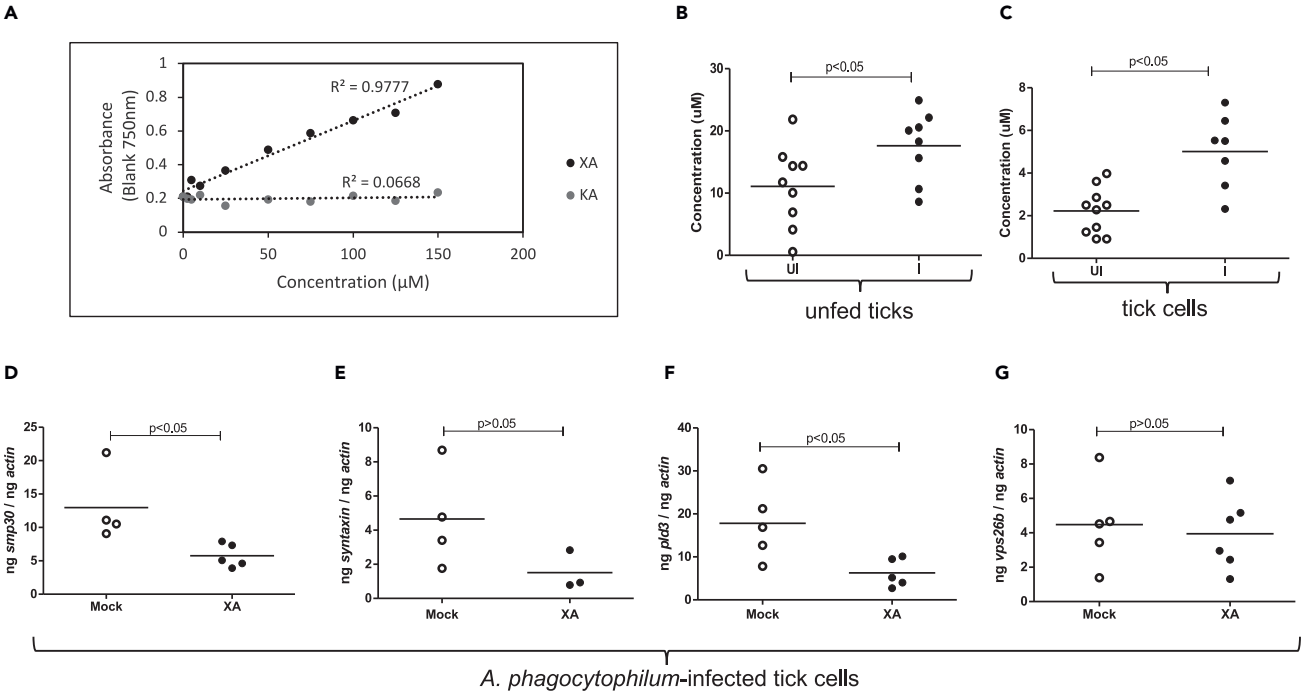

Figure 4. *Anaplasma phagocytophilum* induces production of endogenous XA in ticks and tick cells

(A–G) (A) Graphical representation of the absorbance of XA and KA standards at different concentrations measured at 750 nm. Measurement of endogenous XA levels in uninfected (UI) or *A. phagocytophilum*-infected (I) unfed nymphal ticks (B) or in tick cells (C). Open/closed circles represent data obtained from uninfected (UI)/infected (I) ticks or tick cells, respectively. In B, each circle represents samples generated from pool of five ticks and in C, each circle represents data from one independent culture plate well in a plate. Horizontal lines in the graphs represents mean of the data points. qPCR analysis showing expression of four genes: *smp30* (D), *syntaxin* (E), *pld3* (F), *vps26b* (G) in mock (M)- or xanthurenic acid (XA)-treated *A. phagocytophilum* infected tick cells. In all panels, open circles represent data from mock-treated and closed circles represent data from XA-treated infected tick cells. Each circle represents data from one independent culture plate well in a plate. Horizontal lines in the graphs represents mean of the data points. The mRNA levels of these genes are normalized to tick beta-actin mRNA levels. p value from Student's *t* test is shown.

the levels noted in uninfected controls (Figure 4B). Similarly, we observed significantly ($p < 0.05$) increased levels of endogenous XA levels in *A. phagocytophilum*-infected tick cells when compared to the levels noted in uninfected controls (Figure 4C). These results show that *A. phagocytophilum* significantly increases endogenous levels of tryptophan metabolite, XA, in both ticks and tick cells.

Exogenous treatment with tryptophan metabolite XA down-regulates *smp30 and pld3 gene expression* in *A. phagocytophilum*-infected tick cells

We then studied the mRNA expression levels of cell death marker genes in mock- and XA-treated *A. phagocytophilum*-infected tick cells. qPCR analysis revealed that the expression of *smp30* (Figure 4D) and *pld3* (Figure 4F) transcripts were significantly ($p < 0.05$) decreased in XA-treated *A. phagocytophilum*-infected tick cells in comparison to the levels noted in mock-treated control cells. In addition, we noted significant ($p < 0.05$) downregulation of *caspase* gene expression in *A. phagocytophilum*-infected XA-treated tick cells in comparison to the expression noted in mock-treated controls (Figure S5D). However, no significant differences in the transcript levels of *syntaxin* (Figure 4E) or *vps26b* (Figure 4G) were evident between XA-treated *A. phagocytophilum*-infected tick cells and mock-treated controls. As expected, qPCR analysis confirmed presence of *A. phagocytophilum* in both mock- or XA-treated tick cells (Figure S5E). Collectively, these results suggest that *A. phagocytophilum* modulates expression of some of the tick cell death markers through activation of tryptophan pathway.

Expression of *p38 mapk* is developmentally regulated

Increased phosphorylation of p38 MAPK was shown to be associated with delayed apoptosis in *A. phagocytophilum*-infected human neutrophils.[32] Because we observed increased survival and viability of *A. phagocytophilum*-infected tick cells on XA treatment, we reasoned whether p38 MAPK pathway is activated in *A. phagocytophilum*-infected ticks. We first combed the *I. scapularis* genome, identified tick

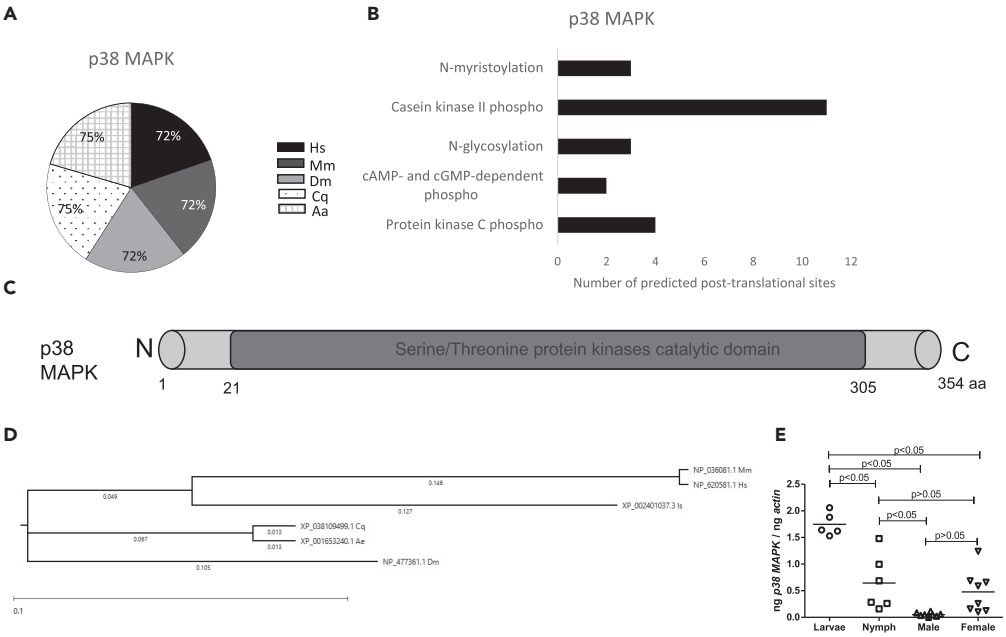

Figure 5. Sequence analysis of *p38 MAPK* and the levels of *p38 mapk* transcripts at different developmental stages of *I. scapularis*

(A) Pie-chart represents percent identify of *I. scapularis* p38 MAPK amino acid sequence with ortholog proteins from *Homo sapiens* (Hs), *Mus musculus* (Mm), *Drosophila melanogaster* (Dm), *Culex quinquefasciatus* (Cq) and *Aedes aegypti* (Aa).

(B) Number of predicted post-translational sites in p38 MAPK protein were analyzed at PROSITE.

(C) Schematic representation of *I. scapularis* p38 MAPK protein structure is shown. Domain analysis of *I. scapularis* p38 MAPK primary amino acid sequence showing presence of serine/threonine protein kinases catalytic domain (21–305 aa).

(D) Sequence analysis of *I. scapularis* p38 MAPK amino acid sequence with other orthologs is shown. The phylogenetic tree was generated in DNASTAR using the Neighbor-Joining (BIONJ) method with BIONJ algorithm.

(E) qPCR analysis showing expression of *p38 MAPK* at different tick developmental stages in uninfected unfed ticks. Each data point in nymphs and adult samples represents transcript levels noted in an individual tick. For larval samples, each data point represents transcript levels noted in 5 pooled larvae. Horizontal lines in the graphs represents mean of the data points. The mRNA levels are normalized to tick beta-actin mRNA levels. Statistical significance was calculated using ANOVA analysis.

p38 MAPK ortholog and performed sequence analysis of tick p38 MAPK. Percent identity of *I. scapularis* p38 MAPK (Figure 5A) amino acid sequence with ortholog proteins from *H. sapiens* (Hs), *M. musculus* (Mm), *D. melanogaster* (Dm), *C. quinquefasciatus* (Cq) and *A. aegypti* (Aa) were determined by CLUSTALW alignment. The *I. scapularis* p38MAPK amino acid sequence shares 72–75% identity with human, mouse, *D. melanogaster*, *C. quinquefasciatus and A. aegypti* p38MAPK orthologs (Figure 5A). Bioinformatic analysis of post translational modification sites in *I. scapularis* p38 MAPK revealed four Protein kinase C phosphorylation sites, two cAMP- and cGMP-dependent protein kinase phosphorylation sites, three N-glycosylation sites, eleven Casein kinase II phosphorylation sites and three N-myristoylation sites (Figure 5B). Domain analysis of *I. scapularis* p38 MAPK primary amino acid sequence showed presence of serine/threonine protein kinases catalytic domain (21–305 aa) (Figure 5C). Sequence analysis showed that *I. scapularis* p38 MAPK fall in a different clade than rest of the orthologs. (Figure 5D). However, *I. scapularis* p38 MAPK forms a clade close to human and mice orthologs (Figure 5D). These analyses reveal that *I. scapularis* p38 MAPK sequence is conserved and retains functional domains that are evident in other orthologs.

We then analyzed the transcript levels of *p38 mapk* at all tick developmental stages (Figure 5E). qPCR analysis showed that larvae expressed significantly ($p < 0.05$) higher levels of *p38 mapk* in comparison to nymph, male and female adult ticks. Nymphs expressed significantly ($p < 0.05$) higher levels of *p38 MAPK* mRNA in comparison to male adult ticks (Figure 5E). No significant ($p > 0.05$) differences in the levels of *p38 mapk* transcripts were noted between nymphs and female ticks or between male and female ticks (Figure 5E). These data show variable expression pattern of *p38 mapk* transcripts at different tick developmental stages.

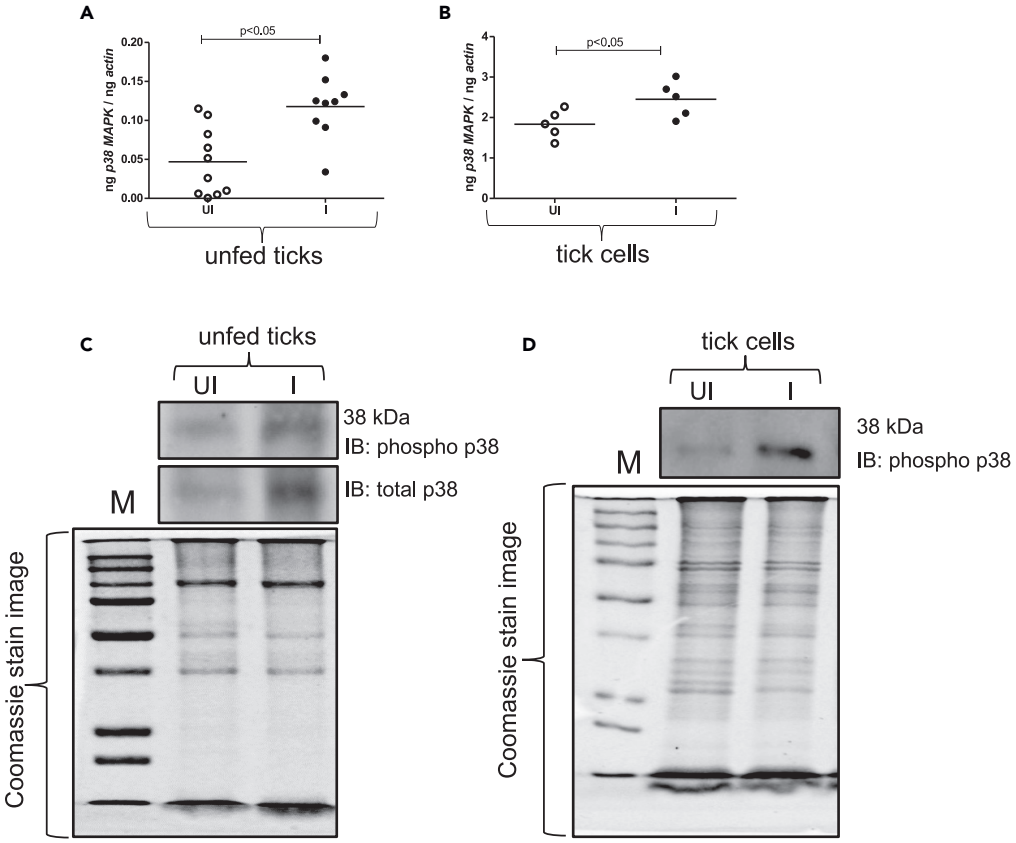

Figure 6. *Anaplasma phagocytophilum* upregulates p38 MAPK levels in unfed nymphal ticks and tick cells

(A and B) Quantitative PCR analysis showing expression of *p38 mapk* in unfed uninfected or *A. phagocytophilum*-infected ticks (A) or tick cells (B). Open circles represent data from uninfected (UI) and closed circles represent data from infected (I) ticks or tick cells. Each circle represents data from one tick (A) or samples collected from one culture plate well in a plate (B). Horizontal lines in the graphs represents mean of the data points. The mRNA levels of these genes were normalized to tick beta-actin mRNA levels. p value from Student's *t* test is shown.

(C) Immunoblotting analysis showing phosphorylated and total p38 MAPK levels in uninfected (UI) or *A. phagocytophilum*-infected (I) unfed nymphal ticks.

(D) Immunoblotting analysis showing phosphorylated p38 MAPK levels in uninfected (UI) or *A. phagocytophilum*-infected (I) tick cells. Coomassie blue stained gel image for total protein profile serves as loading control in the immunoblotting analysis. M indicates Precision Plus protein all blue marker from BioRad, USA.

A. phagocytophilum infection modulates p38 *mapk* expression in ticks and tick cells

We then analyzed whether *A. phagocytophilum* modulates expression of *p38 mapk*. Transcript levels of *p38 mapk* was analyzed in uninfected or *A. phagocytophilum*-infected ticks and tick cells (Figures 6A and 6B). qPCR analysis revealed that expression of *p38 mapk* (Figure 6A) was significantly increased in *A. phagocytophilum*-infected ticks when compared to levels noted in uninfected ticks. Similarly, we also observed increased gene expression of *p38 mapk* in *A. phagocytophilum*-infected tick cells when compared to the levels noted in uninfected controls (Figure 6B). Immunoblotting assay revealed two-three fold increase in both total and phosphorylated p38 MAPK levels in *A. phagocytophilum* infected ticks (Figures 6C, S6A, S6B and Table S3) and tick cells (Figures 6D, S6C and Table S3) in comparison to the levels noted in uninfected controls. These results show that *A. phagocytophilum* upregulate both total and activated p38 MAPK levels in ticks and tick cells.

A. phagocytophilum modulates XA-mediated activation of arthropod p38 MAPK pathway to decrease tick cell death

Because we saw increased *p38 mapk* transcripts and increased total and phosphorylated p38 MAPK levels in *A. phagocytophilum*-infected ticks and tick cells in comparison to their respective uninfected controls,

we analyzed the effect of exogenously added XA on p38 MAPK activation. qPCR analysis revealed no significant differences in the *p38 mapk* transcript levels between mock or XA-treated *A. phagocytophilum*-infected tick cells (Figure 7A). However, immunoblotting assay revealed increased phosphorylation of p38 MAPK in *A. phagocytophilum*-infected XA-treated tick cells when compared to the levels noted in mock-treated controls (Figures 7B, S6C and Table S3). To analyze whether *A. phagocytophilum* and XA concurrently mediates activation of p38 MAPK that prevents tick cell death, we used BIRB796, a pan inhibitor of phosphorylation of all isoforms of p38 MAPK.[41] Treatment of tick cells with different concentrations of BIRB796 revealed inhibition of phosphorylated p38 MAPK levels at 10 and 100 μM (Figures S7 and Table S3). Furthermore, immunoblotting assay revealed decreased levels of phospho-p38 MAPK in both BIRB796-treated uninfected or *A. phagocytophilum*-infected tick cells when compared to respective mock-treated controls (Figures 7C, S8 and Table S3). However, the addition of XA restored activation of p38 MAPK even in the presence of BIRB796 (Figures 7C and S8). Increased phospho-p38 MAPK levels were noted in both uninfected and *A. phagocytophilum*-infected tick cells treated with XA + BIRB796 in comparison to the levels noted in BIRB796-only-treated controls (Figures 7C and S8). In addition, *A. phagocytophilum* burden was noted to be significantly ($p < 0.05$) reduced in BIRB796-treated *A. phagocytophilum*-infected tick cells when compared to the bacterial burden noted in mock-treated control (Figure 7D). However, exogenous treatment with XA significantly ($p < 0.05$) rescued the BIRB796-mediated reduction in bacterial burden (Figure 7D). Furthermore, MTT assay results revealed significantly ($p < 0.05$) decreased *A. phagocytophilum*-infected tick cell viability on treatment with BIRB796 when compared to the viability noted in mock-treated control group (Figure 7E). However, significantly ($p < 0.05$) enhanced cell viability was noted in XA + BIRB796-treated *A. phagocytophilum*-infected cells compared to the viability noted in BIRB796-alone-treated or mock-treated control (Figure 7E). Collectively, these results indicate that *A. phagocytophilum* induced XA-mediated activation of p38 MAPK pathway is important in the inhibition of tick cell death.

DISCUSSION

Induction of host cell death pathways such as apoptosis, pyroptosis, oncosis and autophagy are reported during infection with various pathogens.[30,42] Host cells try to restrict the growth of invading bacteria, viruses, and parasites by inducing cell death pathways that eventually results in the clearance of pathogens.[30,42] However, intracellular pathogens modulate several signaling cascades, including inhibition of cell death pathways, for their survival in the host cells.[4,31,42] In this study, we report a finding that *A. phagocytophilum* inhibits tick cell death by tryptophan metabolite-mediated activation of p38 MAPK.

Previous study from our laboratory has demonstrated that *A. phagocytophilum* modulates the tryptophan pathway and OATP.[17] Both *isoatp4056* and *kat* genes were noted to be upregulated in the salivary glands of *A. phagocytophilum*-infected nymphal ticks.[17] Upregulation of *kat* genes in *A. phagocytophilum*-infected ticks suggested increased production of endogenous XA.[17] The observation of increased XA levels in *A. phagocytophilum*-infected ticks and tick cells in this study corroborates our previous findings. It was reported that the concentration of XA was shown to be increased in mosquito guts after 24 h blood ingestion to millimolar levels.[35] However, mosquitoes fed with sugar were noted to have very low levels of XA.[35] In addition, it has been reported that rat brain regions, such as olfactory bulbs and hippocampus, has XA at a concentration around 1 μM.[43] Authors reasoned that XA at 1 μM level could efficiently participate in signaling in the rat brain.[43] Therefore, observation of low levels of XA in unfed nymphal ticks and tick cells at micromolar levels and its participation in p38-mediated inhibition of cell death in the current study is not surprising.

We selected cell death markers (SMP30, syntaxin, PLD3 and Vps26B) based on the findings from previous studies.[36–39] The amino acid sequences of tick proteins showed higher percent of identity with arthropod orthologs than to human or mouse proteins. The detection of transcripts of these proteins in larvae, nymphs, male and females suggests importance of these proteins at all tick developmental stages. Downregulation of *vps26B* transcript levels in *A. phagocytophilum*-infected tick cells but not in ticks suggest differences in the expression of transcripts between *in vitro* and *in vivo* samples. ISE6 cells were generated from embryonated tick eggs and these cells show neuronal-like phenotype.[44] Studies have noted differences in the expression of several transcripts between ticks and tick cells.[27,45] Therefore, it is not surprising to see the differences in the *vps26B* expression between ticks and tick cells. In addition, observation of no changes in *vps26B* expression in tick cells on XA treatment indicates an XA-independent role for this protein in tick cells.

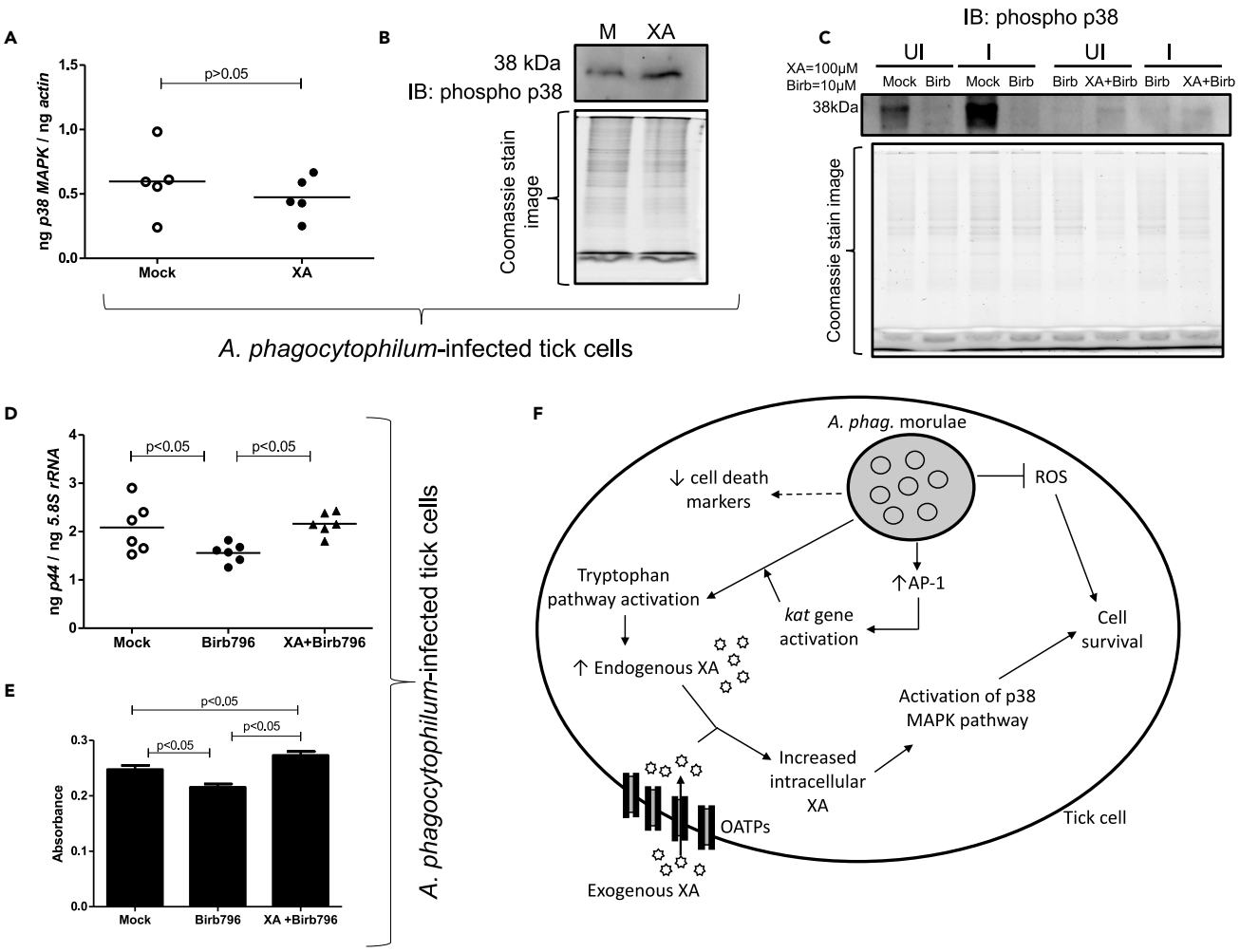

Figure 7. Exogenous addition of Xanthurenic acid increases the expression of *p38 MAPK* mRNA levels and inhibits cell death in *A. phagocytophilum*-infected tick cells

(A) qPCR analysis showing expression of *p38 MAPK* in mock (M)- or xanthurenic acid (XA)-treated *A. phagocytophilum* infected tick cells. Open circles represent data from mock-treated and closed circles represent data from XA-treated infected tick cells. Each circle represents data from one independent culture plate well in a plate. Horizontal lines in the graphs represents mean of the data points. The mRNA levels of these genes are normalized to tick beta-actin mRNA levels. p value from Student's *t* test is shown.

(B) Immunoblotting analysis showing phosphorylated p38 MAPK levels in mock (M)- or XA-treated *A. phagocytophilum* infected tick cells.

(C) Immunoblotting analysis showing phosphorylated p38 MAPK levels in uninfected (UI) or *A. phagocytophilum*-infected (I) tick cells that were treated with mock (M), BIRB796 (Birb), or XA and BIRB796 (XA + Birb). Coomassie blue stained gel image for total protein profile serves as loading control in the immunoblotting analysis.

(D) qPCR analysis showing *A. phagocytophilum* burden in mock, BIRB796 or XA and BIRB796 treated tick cells. Open circles represent data from mock-treated, closed circles represent data from BIRB796-treated and closed triangles represent data from XA and BIRB 796-treated infected tick cells. Each circle and triangle represent data from one independent culture plate well in a plate. Horizontal lines in the graphs represents mean of the data points. The mRNA level of *p44* gene is normalized to tick *5.8S rRNA* levels.

(E) MTT assay results are shown. Absorbance values for mock (M), BIRB796 (Birb), or XA and BIRB796 (XA + Birb) treated *A. phagocytophilum*-infected tick cell samples is shown. For D and E panels, Statistical significance was calculated using ANOVA analysis and p value is shown.

(F) Proposed model on the role of xanthurenic acid in *A. phagocytophilum*-associated modulation of tick cell survival is shown. *Anaplasma phagocytophilum* activates tryptophan metabolism pathway on entry into a tick cell via upregulation of transcription activator protein-1 (AP-1) which results in increased production of endogenous xanthurenic acid (XA) and inhibition of build-up of reactive oxygen species (ROS) production. In addition, organic anion transporting polypeptide will aid in the intake of exogenous XA. Both endogenous and exogenous XA activates p38 MAPK signaling. In addition, *A. phagocytophilum* infection results in the downregulation of cell death markers that suggests reduced tick cell death. XA-mediated activation of p38 MAPK signaling results in increased tick cell survival that eventually favors extended bacterial colonization it their vector. Picture is not drawn to the scale.

P38 MAPK is involved in various cellular processes including differentiation, inflammation, proliferation and cell survival.[46] The observation of increased *p38 mapk* transcripts in larval stages when compared to the levels noted in nymphs or adult stages suggests an important role for this global regulator in the immature stages of ticks. Larval ticks take a blood meal to molt to nymphal stages. Increased level of P38 MAPK could facilitate inhibition of cell death during molting of these immature ticks to the nymphal stages. Sequence analysis revealed that tick p38 MAPK was close to several arthropod orthologs and to human and mouse counterparts. Several studies have shown that multiple signaling pathways (p38 MAPK, PI3K, p42/44 ERK) can delay apoptosis in human neutrophils.[47–50] The presence of conserved serine/threonine protein kinase catalytic domain and high percentage of amino acid sequence identity with mammalian orthologs suggests that arthropod p38 MAPK could also function in various cellular signaling events in ticks. p38 MAPK is activated by phosphorylation. The presence of several phosphorylation sites on tick p38 MAPK (Figure 5B) and its detection with phospho-p38 MAPK antibody indicates activation of tick p38 MAPK by phosphorylation. The phospho-p38 MAPK antibody used in this study recognizes phosphorylated sites on human p38 MAPK at Thr180/Tyr182. These residues are Thr177/Tyr179 in tick p38 MAPK suggesting conserved phosphorylation pattern for the activation of this kinase. BIRB796 is a potent inhibitor of all isoforms of p38 MAPK.[41] The observation of significantly reduced levels of phospho-p38 MAPK in BIRB796-treated tick cells suggests that these residues are critical for tick p38 MAPK activation.

It has also been reported that p38 MAPK mediates mammalian cell survival by protecting them from ROS accumulation.[51] Authors noted that p38 MAPK increases expression of antioxidant enzymes: superoxide-dismutase 1 (SOD-1), SOD-2 and catalase by various mechanisms to protect from ROS damage.[51] In our previous study, we reported observation of increased ROS production on *A. phagocytophilum*-infection of tick cells.[18] However, exogenous addition of XA inhibited build-up of ROS levels.[18] In addition, we noted that RNAi-mediated knockdown of *kat* gene expression resulted in increased ROS production that eventually resulted in bacterial clearance.[18] In this study, the observation of increased phosphorylated levels of p38 MAPK levels in the presence of *A. phagocytophilum* and/or XA indicate that this bacterium modulates tryptophan pathway to activate p38 MAPK pathway for inhibiting buildup of ROS levels and preventing tick cell death. We recently reported that *A. phagocytophilum* upregulates activator protein-1 (AP-1) to activate *kat* gene promoter.[16] KAT is an enzyme that catalyzes production of XA. Therefore, we believe that *A. phagocytophilum* induces synthesis of XA by upregulating AP-1 gene expression. In addition, p38 MAPK is noted to activate AP-1.[52] The observation of increased transcript and protein levels for total p38 MAPK in *A. phagocytophilum*-infected ticks suggests that this bacterium modulates a feedback mechanism to concurrently regulate tryptophan and p38 MAPK pathways via AP-1 for its survival in the vector host cells.

Based on the observations from our previous[16–18] and current study, we propose a model on how *A. phagocytophilum* inhibits tick cell death (Figure 7F). *A. phagocytophilum* enters tick cells and multiply in a host-derived vacuole (Figure 7F). On entry into tick cells, *A. phagocytophilum* upregulates OATP and AP-1 that activates tryptophan pathway to increase endogenous levels of XA leading to the inhibition of build-up of reactive oxygen species (ROS) production (Figure 7F). Increased OATP levels could lead to transport of more exogenous XA in to tick cells (Figure 7F). The increased levels of endogenous and exogenous XA activates p38 MAPK pathway leading to the inhibition of tick cell death. Downregulation of cell death markers further indicates reduced cell death in *A. phagocytophilum*-infected tick cells.

In summary, we provide evidence that *A. phagocytophilum* not only modulates tryptophan-metabolite mediated activation of p38 MAPK but also delineates that activation of these pathways are critical for the survival of both this bacterium and its vector host. Studies like these are important to understand how intracellular rickettsial pathogens modulate cell signaling for their survival in the vector host.

Limitations of the study

In this study, we provide an evidence on how an intracellular bacterial pathogen modulates two important arthropod pathways (tryptophan and p38 MAPK) for its survival in ticks. One of the limitations of this study is the lack of using *p38 mapk* or *kat* gene knockout ticks and studying tick cell survival. Although the tools for generating tick gene knockouts are emerging, they are very laborious and not routinely used. The other limitation of this study is, we did not address whether changes in tryptophan and p38 MAPK pathways are directly regulated by the bacteria. *A. phagocytophilum* secretes several effector proteins into the

host cell. Therefore, more work is needed to address whether tick cell survival is directly regulated by *A. phagocytophilum* effector proteins.

STAR★METHODS

Detailed methods are provided in the online version of this paper and include the following:

- KEY RESOURCES TABLE
- RESOURCE AVAILABILITY
  - Lead contact
  - Materials availability
  - Data and code availability
- EXPERIMENTAL MODEL AND SUBJECT DETAILS
  - Bacteria
  - Ticks
  - Tick cell line
- METHOD DETAILS
  - Mice and tick feeding
  - Ethics statement
  - Total RNA, DNA isolation and qPCR data analysis
  - Tick cell line experiments with xanthurenic acid (XA)
  - Tick cell line experiments with BIRB796, the p38 MAPK inhibitor
  - Live/dead assay
  - MTT assay
  - Western blotting assay
  - Endogenous XA measurement
  - Sequence alignment and analysis
- QUANTIFICATION AND STATISTICAL ANALYSIS

SUPPLEMENTAL INFORMATION

Supplemental information can be found online at https://doi.org/10.1016/j.isci.2022.105730.

ACKNOWLEDGMENTS

The following reagents were provided by Centers for Disease Control and Prevention for distribution by BEI Resources, NIAID, NIH: *Ixodes scapularis* Adult (Live), NR-42510, Larvae (Live), NR-44115 and Nymph (Live), NR-44116. The following reagent was obtained through BEI Resources, NIAID, NIH: *Anaplasma phagocytophilum*, Strain NCH-1, NR-48807. This study was supported by funding from National Institute of Allergy and Infectious Diseases (NIAID), National Institutes of Healthh (NIH) (Award number: R01AI130116) to G.N. and University of Tennessee, Knoxville, Start-up funds to H.S. and G.N.

AUTHOR CONTRIBUTIONS

P.N., M.D., and G.N. performed the experiments. P.N., M.D., H.S., and G.N. analyzed the data. P.N., H.S., and G.N. designed the study, H.S. and G.N. provided reagents. All authors read, edited, and approved the manuscript. P.N. and G.N. wrote the paper. G.N. conceptualized and conceived the study and supervised overall investigations.

DECLARATION OF INTERESTS

The authors declare no competing interests.

Received: July 29, 2022
Revised: October 27, 2022
Accepted: December 1, 2022
Published: January 20, 2023

REFERENCES

1. de la Fuente, J., Estrada-Pena, A., Venzal, J.M., Kocan, K.M., and Sonenshine, D.E. (2008). Overview: ticks as vectors of pathogens that cause disease in humans and animals. Front. Biosci. *13*, 6938–6946. https://doi.org/10.2741/3200.

2. Neelakanta, G., and Sultana, H. (2015). Transmission-blocking vaccines: focus on anti-vector vaccines against tick-borne diseases. Arch. Immunol. Ther. Exp. *63*, 169–179. https://doi.org/10.1007/s00005-014-0324-8.

3. Pusterla, N., Chae, J.S., Kimsey, R.B., Berger Pusterla, J., DeRock, E., Dumler, J.S., and Madigan, J.E. (2002). Transmission of Anaplasma phagocytophila (human granulocytic ehrlichiosis agent) in horses using experimentally infected ticks (Ixodes scapularis). J. Vet. Med. B Infect. Dis. Vet. Public Health *49*, 484–488. https://doi.org/10.1046/j.1439-0450.2002.00598.x.

4. Rikihisa, Y. (2011). Mechanisms of obligatory intracellular infection with Anaplasma phagocytophilum. Clin. Microbiol. Rev. *24*, 469–489. https://doi.org/10.1128/cmr.00064-10.

5. Zeman, P., Januska, J., Orolinova, M., Stuen, S., Struhar, V., and Jebavy, L. (2004). High seroprevalence of granulocytic ehrlichiosis distinguishes sheep that were the source of an alimentary epidemic of tick-borne encephalitis. Wien Klin. Wochenschr. *116*, 614–616. https://doi.org/10.1007/s00508-004-0191-0.

6. Anderson, J.F., and Magnarelli, L.A. (2008). Biology of ticks. Infect. Dis. Clin. North Am. *22*, 195–215. https://doi.org/10.1016/j.idc.2007.12.006.

7. Hodzic, E., Fish, D., Maretzki, C.M., De Silva, A.M., Feng, S., and Barthold, S.W. (1998). Acquisition and transmission of the agent of human granulocytic ehrlichiosis by Ixodes scapularis ticks. J. Clin. Microbiol. *36*, 3574–3578. https://doi.org/10.1128/jcm.36.12.3574-3578.1998.

8. Chen, S.M., Dumler, J.S., Bakken, J.S., and Walker, D.H. (1994). Identification of a granulocytotropic Ehrlichia species as the etiologic agent of human disease. J. Clin. Microbiol. *32*, 589–595. https://doi.org/10.1128/jcm.32.3.589-595.1994.

9. Bakken, J.S., and Dumler, J.S. (2015). Human granulocytic anaplasmosis. Infect. Dis. Clin. North Am. *29*, 341–355. https://doi.org/10.1016/j.idc.2015.02.007.

10. Carlyon, J.A., and Fikrig, E. (2003). Invasion and survival strategies of Anaplasma phagocytophilum. Cell Microbiol. *5*, 743–754. https://doi.org/10.1046/j.1462-5822.2003.00323.x.

11. Niu, H., Xiong, Q., Yamamoto, A., Hayashi-Nishino, M., and Rikihisa, Y. (2012). Autophagosomes induced by a bacterial Beclin 1 binding protein facilitate obligatory intracellular infection. Proc. Natl. Acad. Sci. USA *109*, 20800–20807. https://doi.org/10.1073/pnas.1218674109.

12. Truchan, H.K., Cockburn, C.L., Hebert, K.S., Magunda, F., Noh, S.M., and Carlyon, J.A. (2016). The pathogen-occupied vacuoles of Anaplasma phagocytophilum and Anaplasma marginale interact with the endoplasmic reticulum. Front. Cell. Infect. Microbiol. *6*, 22. https://doi.org/10.3389/fcimb.2016.00022.

13. Truchan, H.K., VieBrock, L., Cockburn, C.L., Ojogun, N., Griffin, B.P., Wijesinghe, D.S., Chalfant, C.E., and Carlyon, J.A. (2016). Anaplasma phagocytophilum Rab10-dependent parasitism of the trans-Golgi network is critical for completion of the infection cycle. Cell Microbiol. *18*, 260–281. https://doi.org/10.1111/cmi.12500.

14. Garcia-Garcia, J.C., Barat, N.C., Trembley, S.J., and Dumler, J.S. (2009). Epigenetic silencing of host cell defense genes enhances intracellular survival of the rickettsial pathogen Anaplasma phagocytophilum. PLoS Pathog. *5*, e1000488. https://doi.org/10.1371/journal.ppat.1000488.

15. Lin, M., and Rikihisa, Y. (2003). Ehrlichia chaffeensis and Anaplasma phagocytophilum lack genes for lipid A biosynthesis and incorporate cholesterol for their survival. Infect. Immun. *71*, 5324–5331. https://doi.org/10.1128/iai.71.9.5324-5331.2003.

16. Khanal, S., Taank, V., Anderson, J.F., Sultana, H., and Neelakanta, G. (2018). Arthropod transcriptional activator protein-1 (AP-1) aids tick-rickettsial pathogen survival in the cold. Sci. Rep. *8*, 11409. https://doi.org/10.1038/s41598-018-29654-6.

17. Taank, V., Dutta, S., Dasgupta, A., Steeves, T.K., Fish, D., Anderson, J.F., Sultana, H., and Neelakanta, G. (2017). Human rickettsial pathogen modulates arthropod organic anion transporting polypeptide and tryptophan pathway for its survival in ticks. Sci. Rep. *7*, 13256. https://doi.org/10.1038/s41598-017-13559-x.

18. Dahmani, M., Anderson, J.F., Sultana, H., and Neelakanta, G. (2020). Rickettsial pathogen uses arthropod tryptophan pathway metabolites to evade reactive oxygen species in tick cells. Cell Microbiol. *22*, e13237. https://doi.org/10.1111/cmi.13237.

19. Ramasamy, E., Taank, V., Anderson, J.F., Sultana, H., and Neelakanta, G. (2020). Repression of tick microRNA-133 induces organic anion transporting polypeptide expression critical for Anaplasma phagocytophilum survival in the vector and transmission to the vertebrate host. PLoS Genet. *16*, e1008856. https://doi.org/10.1371/journal.pgen.1008856.

20. Neelakanta, G., Sultana, H., Fish, D., Anderson, J.F., and Fikrig, E. (2010). Anaplasma phagocytophilum induces Ixodes scapularis ticks to express an antifreeze glycoprotein gene that enhances their survival in the cold. J. Clin. Invest. *120*, 3179–3190. https://doi.org/10.1172/jci42868.

21. Sultana, H., Neelakanta, G., Kantor, F.S., Malawista, S.E., Fish, D., Montgomery, R.R., and Fikrig, E. (2010). Anaplasma phagocytophilum induces actin phosphorylation to selectively regulate gene transcription in Ixodes scapularis ticks. J. Exp. Med. *207*, 1727–1743. https://doi.org/10.1084/jem.20100276.

22. Liu, L., Dai, J., Zhao, Y.O., Narasimhan, S., Yang, Y., Zhang, L., and Fikrig, E. (2012). Ixodes scapularis JAK-STAT pathway regulates tick antimicrobial peptides, thereby controlling the agent of human granulocytic anaplasmosis. J. Infect. Dis. *206*, 1233–1241. https://doi.org/10.1093/infdis/jis484.

23. Ayllón, N., Villar, M., Busby, A.T., Kocan, K.M., Blouin, E.F., Bonzón-Kulichenko, E., Galindo, R.C., Mangold, A.J., Alberdi, P., Pérez de la Lastra, J.M., et al. (2013). Anaplasma phagocytophilum inhibits apoptosis and promotes cytoskeleton rearrangement for infection of tick cells. Infect. Immun. *81*, 2415–2425. https://doi.org/10.1128/iai.00194-13.

24. Khanal, S., Taank, V., Anderson, J.F., Sultana, H., and Neelakanta, G. (2022). Rickettsial pathogen perturbs tick circadian gene to infect the vertebrate host. Int. J. Mol. Sci. *23*, 3545.

25. Turck, J.W., Taank, V., Neelakanta, G., and Sultana, H. (2019). Ixodes scapularis Src tyrosine kinase facilitates Anaplasma phagocytophilum survival in its arthropod vector. Ticks Tick. Borne. Dis. *10*, 838–847. https://doi.org/10.1016/j.ttbdis.2019.04.002.

26. Alberdi, P., Espinosa, P.J., Cabezas-Cruz, A., and de la Fuente, J. (2016). Anaplasma phagocytophilum manipulates host cell apoptosis by different mechanisms to establish infection. Vet. Sci. *3*, 15. https://doi.org/10.3390/vetsci3030015.

27. Alberdi, P., Cabezas-Cruz, A., Prados, P.E., Rayo, M.V., Artigas-Jerónimo, S., and de la Fuente, J. (2019). The redox metabolic pathways function to limit Anaplasma phagocytophilum infection and multiplication while preserving fitness in tick vector cells. Sci. Rep. *9*, 13236. https://doi.org/10.1038/s41598-019-49766-x.

28. Artigas-Jerónimo, S., Alberdi, P., Villar Rayo, M., Cabezas-Cruz, A., Prados, P.J.E., Mateos-Hernández, L., and de la Fuente, J. (2019). Anaplasma phagocytophilum modifies tick cell microRNA expression and upregulates isc-mir-79 to facilitate infection by targeting the Roundabout protein 2 pathway. Sci. Rep. *9*, 9073. https://doi.org/10.1038/s41598-019-45658-2.

29. Shaw, D.K., Wang, X., Brown, L.J., Chávez, A.S.O., Reif, K.E., Smith, A.A., Scott, A.J., McClure, E.E., Boradia, V.M., Hammond, H.L., et al. (2017). Infection-derived lipids elicit an immune deficiency circuit in arthropods. Nat. Commun. *8*, 14401. https://doi.org/10.1038/ncomms14401.

30. Labbé, K., and Saleh, M. (2008). Cell death in the host response to infection. Cell Death Differ. *15*, 1339–1349. https://doi.org/10.1038/cdd.2008.91.

31. Rikihisa, Y. (2010). Anaplasma phagocytophilum and Ehrlichia chaffeensis: subversive manipulators of host cells. Nat. Rev. Microbiol. *8*, 328–339. https://doi.org/10.1038/nrmicro2318.

32. Choi, K.S., Park, J.T., and Dumler, J.S. (2005). Anaplasma phagocytophilum delay of neutrophil apoptosis through the p38 mitogen-activated protein kinase signal pathway. Infect. Immun. *73*, 8209–8218. https://doi.org/10.1128/iai.73.12.8209-8218.2005.

33. Billker, O., Lindo, V., Panico, M., Etienne, A.E., Paxton, T., Dell, A., Rogers, M., Sinden, R.E., and Morris, H.R. (1998). Identification of xanthurenic acid as the putative inducer of malaria development in the mosquito. Nature *392*, 289–292. https://doi.org/10.1038/32667.

34. Garcia, G.E., Wirtz, R.A., Barr, J.R., Woolfitt, A., and Rosenberg, R. (1998). Xanthurenic acid induces gametogenesis in Plasmodium, the malaria parasite. J. Biol. Chem. *273*, 12003–12005. https://doi.org/10.1074/jbc.273.20.12003.

35. Lima, V.L.A., Dias, F., Nunes, R.D., Pereira, L.O., Santos, T.S.R., Chiarini, L.B., Ramos, T.D., Silva-Mendes, B.J., Perales, J., Valente, R.H., and Oliveira, P.L. (2012). The antioxidant role of xanthurenic acid in the Aedes aegypti midgut during digestion of a blood meal. PLoS One *7*, e38349. https://doi.org/10.1371/journal.pone.0038349.

36. Khang, R., Jo, A., Kang, H., Kim, H., Kwag, E., Lee, J.-Y., Koo, O., Park, J., Kim, H.K., Jo, D.-G., et al. (2021). Loss of zinc-finger protein 212 leads to Purkinje cell death and locomotive abnormalities with phospholipase D3 downregulation. Sci. Rep. *11*, 22745. https://doi.org/10.1038/s41598-021-02218-x.

37. Fujita, T., Inoue, H., Kitamura, T., Sato, N., Shimosawa, T., and Maruyama, N. (1998). Senescence marker protein-30 (SMP30) rescues cell death by enhancing plasma membrane Ca(2+)-pumping activity in Hep G2 cells. Biochem. Biophys. Res. Commun. *250*, 374–380. https://doi.org/10.1006/bbrc.1998.9327.

38. Yeh, C.-Y., Bulas, A.M., Moutal, A., Saloman, J.L., Hartnett, K.A., Anderson, C.T., Tzounopoulos, T., Sun, D., Khanna, R., and Aizenman, E. (2017). Targeting a potassium channel/syntaxin interaction ameliorates cell death in ischemic stroke. J. Neurosci. *37*, 5648–5658. https://doi.org/10.1523/jneurosci.3811-16.2017.

39. Wang, H., Qi, W., Zou, C., Xie, Z., Zhang, M., Naito, M.G., Mifflin, L., Liu, Z., Najafov, A., Pan, H., et al. (2021). NEK1-mediated retromer trafficking promotes blood–brain barrier integrity by regulating glucose metabolism and RIPK1 activation. Nat. Commun. *12*, 4826. https://doi.org/10.1038/s41467-021-25157-7.

40. Ohtsuki, E., Suzuki, M., Takayanagi, M., and Yashiro, T. (1994). Colorimetric determination of urinary xanthurenic acid using an oxidative coupling reaction with N, N-diethyl-p-phenylenediamine. Biol. Pharm. Bull. *17*, 139–141. https://doi.org/10.1248/bpb.17.139.

41. Kuma, Y., Sabio, G., Bain, J., Shpiro, N., Márquez, R., and Cuenda, A. (2005). BIRB796 inhibits all p38 MAPK isoforms in vitro and in vivo. J. Biol. Chem. *280*, 19472–19479. https://doi.org/10.1074/jbc.M414221200.

42. Loterio, R.K., Zamboni, D.S., and Newton, H.J. (2021). Keeping the host alive - lessons from obligate intracellular bacterial pathogens. Pathog. Dis. *79*, ftab052. https://doi.org/10.1093/femspd/ftab052.

43. Gobaille, S., Kemmel, V., Brumaru, D., Dugave, C., Aunis, D., and Maitre, M. (2008). Xanthurenic acid distribution, transport, accumulation and release in the rat brain. J. Neurochem. *105*, 982–993. https://doi.org/10.1111/j.1471-4159.2008.05219.x.

44. Oliver, J.D., Chávez, A.S.O., Felsheim, R.F., Kurtti, T.J., and Munderloh, U.G. (2015). An Ixodes scapularis cell line with a predominantly neuron-like phenotype. Exp. Appl. Acarol. *66*, 427–442. https://doi.org/10.1007/s10493-015-9908-1.

45. Cabezas-Cruz, A., Espinosa, P.J., Obregón, D.A., Alberdi, P., and de la Fuente, J. (2017). Ixodes scapularis tick cells control Anaplasma phagocytophilum infection by increasing the synthesis of phosphoenolpyruvate from tyrosine. Front. Cell. Infect. Microbiol. *7*, 375. https://doi.org/10.3389/fcimb.2017.00375.

46. Cuenda, A., and Rousseau, S. (2007). p38 MAP-kinases pathway regulation, function and role in human diseases. Biochim. Biophys. Acta *1773*, 1358–1375. https://doi.org/10.1016/j.bbamcr.2007.03.010.

47. Alvarado-Kristensson, M., Melander, F., Leandersson, K., Rönnstrand, L., Wernstedt, C., and Andersson, T. (2004). p38-MAPK signals survival by phosphorylation of caspase-8 and caspase-3 in human neutrophils. J. Exp. Med. *199*, 449–458. https://doi.org/10.1084/jem.20031771.

48. Alvarado-Kristensson, M., Porn-Ares, M.I., Grethe, S., Smith, D., Zheng, L., and Andersson, T. (2002). p38 Mitogen-activated protein kinase and phosphatidylinositol 3-kinase activities have opposite effects on human neutrophil apoptosis. FASEB J. *16*, 129–131. https://doi.org/10.1096/fj.01-0817fje.

49. Klein, J.B., Buridi, A., Coxon, P.Y., Rane, M.J., Manning, T., Kettritz, R., and McLeish, K.R. (2001). Role of extracellular signal-regulated kinase and phosphatidylinositol-3 kinase in chemoattractant and LPS delay of constitutive neutrophil apoptosis. Cell. Signal. *13*, 335–343. https://doi.org/10.1016/s0898-6568(01)00151-6.

50. Klein, J.B., Rane, M.J., Scherzer, J.A., Coxon, P.Y., Kettritz, R., Mathiesen, J.M., Buridi, A., and McLeish, K.R. (2000). Granulocyte-macrophage colony-stimulating factor delays neutrophil constitutive apoptosis through phosphoinositide 3-kinase and extracellular signal-regulated kinase pathways. J. Immunol. *164*, 4286–4291. https://doi.org/10.4049/jimmunol.164.8.4286.

51. Gutiérrez-Uzquiza, Á., Arechederra, M., Bragado, P., Aguirre-Ghiso, J.A., and Porras, A. (2012). p38alpha mediates cell survival in response to oxidative stress via induction of antioxidant genes: effect on the p70S6K pathway. J. Biol. Chem. *287*, 2632–2642. https://doi.org/10.1074/jbc.M111.323709.

52. Zarubin, T., and Han, J. (2005). Activation and signaling of the p38 MAP kinase pathway. Cell Res. *15*, 11–18. https://doi.org/10.1038/sj.cr.7290257.

53. Taank, V., Zhou, W., Zhuang, X., Anderson, J.F., Pal, U., Sultana, H., and Neelakanta, G. (2018). Characterization of tick organic anion transporting polypeptides (OATPs) upon bacterial and viral infections. Parasit. Vectors *11*, 593. https://doi.org/10.1186/s13071-018-3160-6.

54. Zhou, W., Woodson, M., Sherman, M.B., Neelakanta, G., and Sultana, H. (2019). Exosomes mediate Zika virus transmission through SMPD3 neutral Sphingomyelinase in cortical neurons. Emerg. Microbes Infect. *8*, 307–326. https://doi.org/10.1080/22221751.2019.1578188.

55. Neelakanta, G., Sultana, H., Sonenshine, D.E., and Andersen, J.F. (2018). Identification and characterization of a histamine-binding lipocalin-like molecule from the relapsing fever tick Ornithodoros turicata. Insect Mol. Biol. *27*, 177–187. https://doi.org/10.1111/imb.12362.

56. Sultana, H., Patel, U., Sonenshine, D.E., and Neelakanta, G. (2015). Identification and comparative analysis of subolesin/akirin ortholog from Ornithodoros turicata ticks. Parasit. Vectors *8*, 132. https://doi.org/10.1186/s13071-015-0749-x.

57. Sultana, H., Patel, U., Toliver, M., Maggi, R.G., and Neelakanta, G. (2016). Molecular identification and bioinformatics analysis of a potential anti-vector vaccine candidate, 15-kDa salivary gland protein (Salp15), from Ixodes affinis ticks. Ticks Tick. Borne. Dis. *7*, 46–53. https://doi.org/10.1016/j.ttbdis.2015.08.003.

STAR★METHODS

KEY RESOURCES TABLE

REAGENT or RESOURCE	SOURCE	IDENTIFIER
Antibodies		
Anti-PLD3	ThermoFisher Scientific	Cat # PIPA5104016; RRID:AB_2853347
Anti- phospho-p38	Cell Signaling Technologies	Cat # 9211S; RRID:AB_331641
Total-p38	Cell Signaling Technologies	Cat # 9212; RRID:AB_330713
HRP-conjugated goat anti-rabbit secondary antibody	Cell Signaling Technologies	Cat #7074S; RRID:AB_2099233
Bacterial and virus strains		
Anaplasma phagocytophilum isolate NCH-1	BEI Resources, NIAID, NIH	NR-48807
Biological samples		
Ixodes scapularis (larvae, nymph, adult male and females)	BEI Resources, NIAID, NIH	NR-44115, NR-42510, NR-44116
Chemicals, peptides, and recombinant proteins		
Potassium sulfate	Alfa Aesar	Cat # A13975
IMDM media	Fisher Scientific	Cat # SH3025901
L-glutamine	Gibco, USA	Cat # 25030-081
FBS	VWR, USA	Cat # 89510-186
Leibovitz's L-15 Medium, powder	Gibco	Cat # 41300-039
Tryptose phosphate broth	MP Biomedicals, USA	Cat # ICN1682149
Bovine Cholesterol Lipoprotein Concentrate:	MP Biomedicals, USA	Cat # ICN19147625
Xanthurenic acid (XA)	Sigma, USA	Cat #D120804-5G
Sodium hydroxide	VWR	Cat # 1310-73-2
DMSO	Sigma, USA	Cat #D5879-500 ML
BIRB796	Tocris, USA	Cat # 59-891-0
MTT (Thiazolyl Blue Tetrazolium Bromide)	Sigma, USA	Cat # MKCR0748
RIPA lysis buffer	BioSciences, USA	Cat # 786-490
EDTA-free protease inhibitor cocktail	Roche	Cat # 11836170001
Laemmli sample buffer	BioRad	Cat # 161-0737
30% Acrylamide	BioRad, USA	Cat # 1610156
SDS	Sigma, USA	Cat #L3771-500G
APS	Columbus Chemical industries, USA	Cat # 053500
Tris HCl	American Bioanalytical	Cat # AB02005-01000
Tris base	Sigma, USA	Cat #T6066-1 KG
Glycine	Sigma, USA	Cat #G8898-1 KG
Hydrochloric acid (HCl)	Macron fine chemicals	Cat #H613-46
Coomassie Blue	BioRad, USA	Cat # 1610400
Nitrocellulose membrane	Amersham GE	Cat # 10600002
BSA	Sigma, USA	Cat # 9048-46-8
Tween 20	American Bioanalytical	Cat # AB02038-00500
Clarity Western ECL substrate	BioRad, USA	Cat # 1705061
Acetate Buffer	ThermoScientific, USA	Cat #J60964.AK
iTaq Universal SYBR Green Supermix	BioRad, USA	Cat #L001752 B
2X Universal SYBR Green fast qPCR Mix	ABclonal, USA	Cat # RM21203

(*Continued on next page*)

Continued

REAGENT or RESOURCE	SOURCE	IDENTIFIER
N, *N*-diethyl-*p*-phenylenediamine (DE-PPD)	Alfa Aesar	Cat # A17832
Horseradish peroxidase (POD)	ThermoScientific, USA	Cat #J60026.MC
Kynurenic acid (KA)	Sigma, USA	Cat #K3375-1G
Hydrogen peroxide	ThermoScientific, USA	Cat # BP2633-500
Protein Plus ladder	BioRad, USA	Cat # 1610373
Critical commercial assays		
Aurum Total RNA Mini kit	BioRad, USA	Cat # 732-6820
DNeasy Blood & Tissue Kit	Qiagen	Cat # 69506
iScript cDNA synthesis kit	BioRad, USA	Cat # 1708891
Bradford (BCA) protein assay kit	Pierce/ThermoScientific, USA	Cat # 23227
LIVE/DEAD Cell Imaging kit	ThermoFisher Scientific	Cat #R37601
Experimental models: Cell lines		
Tick cell line ISE6	ATCC	Cat # CRL-11974
Experimental models: Organisms/strains		
Ticks- *Ixodes scapularis*	BEI Resources, NIAID, NIH	NR-44115, NR-42510, NR-44116
Mice C57BL/6J	Jackson Laboratories, USA	Cat # 000664
Mice B6.129S7-Rag1tm1Mom/J ($RAG^{-/-}$)	Jackson Laboratories, USA	Cat # 002216
Oligonucleotides		
Primers for qPCR	This paper	Integrated DNA Technology
Primers for RNAi analysis	This paper	Integrated DNA Technology
Software and algorithms		
GraphPad Prism	GraphPad, USA	Version 6
ImageJ	ImageJ, NIH	https://imagej.nih.gov/ij/index.html
DNASTAR CLUSTALW alignment	DNASTAR, USA	Lasergene 17

RESOURCE AVAILABILITY

Lead contact

Further information about the protocols and requests for resources and reagents should be directed to and will be fulfilled by the lead contact, Girish Neelakanta (gneelaka@utk.edu).

Materials availability

This study did not generate new unique reagents.

Data and code availability

This paper does not report original code. Any additional information is available from the Lead contact upon request.

EXPERIMENTAL MODEL AND SUBJECT DETAILS

Bacteria

A. phagocytophilum isolate NCH-1 (obtained from BEI Resources, NIAID, NIH), referred to as *A. phagocytophilum*, was used throughout this study. *A. phagocytophilum* was maintained in HL-60 cells and isolated from these cells.[16,17,19] Briefly, infected HL-60 cells were centrifuged for 10 min at 2950 × g at 4°C and the pellet was washed two times with sterile 1XPBS. Cells were then re-suspended in 1× IMDM medium and processed for a freeze/thaw cycle followed by passing through 25- and 27-gauge needles for 6–8 times. The obtained solution was later centrifuged at 260 × g for 3 min to obtain host cell free bacteria in supernatant. This supernatant was used for infection.

Ticks

I. scapularis ticks (larvae, nymphs, adult male and females) used in this study were obtained from BEI Resources, NIAID, NIH. Tick rearing was conducted in laboratory humidity chambers consisting of rubber maid tubs with potassium sulfate and water to raise the humidity to saturation point. The bottom of the humidity chamber was covered with potassium sulfate and 1 inch of water was added above that. Tick vials were placed on the top of the rack and were kept out of this solution. Ticks were held at 73°F.

Tick cell line

The *I. scapularis* tick cell line, ISE6, purchased from ATCC, was grown in L15B300 medium prepared from Leibovitz's L-15 Medium, powder with 5% tryptose phosphate broth, 5% heat-inactivated FBS, and 0.1% bovine lipoprotein concentrate, pH 7.2. ISE6 cultures were maintained at 34°C.[16,17]

METHOD DETAILS

Mice and tick feeding

C57BL/6J and B6.129S7-Rag1tm1Mom/J ($RAG^{-/-}$) (female, 4–6 weeks, Jackson Laboratories, USA) mice were used in this study. *A. phagocytophilum* infection was maintained in B6.129S7-Rag1tm1Mom/J ($RAG^{-/-}$) mice. Uninfected larval ticks were fed on either uninfected or *A. phagocytophilum*-infected mice and were molted to nymphs. Unfed uninfected or *A. phagocytophilum*-infected nymphal ticks were processed for DNA, RNA or protein extractions and were used for Quantitative real-time PCR analysis, immunoblotting and ELISAs.

Ethics statement

All animal experiments performed in this study are in accordance with University of Tennessee, Knoxville Institutional Animal Care and Use Committee (IACUC, animal assurance number: D16-00397) approved protocol 2801–0221. Acepromazine, as a tranquilizer was administered to animals prior to placement of ticks on mice and all efforts were made to minimize suffering.

Total RNA, DNA isolation and qPCR data analysis

Total RNA from ticks (unfed/fed) nymphs and tick cells (2×10^5) was extracted using Aurum Total RNA Mini kit (BioRad, USA) following manufacturer instructions.[18,19,53] The cDNA was generated from total RNA using iScript cDNA synthesis kit (BioRad, USA),[18,19,53] and used as template for the amplification of *smp30*, *pld3*, *syntaxin*, *vps26b* and housekeeping genes (tick beta actin and 5.8S rRNA). DNA from ticks, tick cells and murine tissues were extracted using DNeasy blood and tissue kit (Qiagen, USA). All oligonucleotides used in this study are mentioned in Table S4. qPCR was performed using iQ-SYBR Green Supermix (BioRad, USA) or 2X Universal SYBR Green fast qPCR Mix (ABclonal, USA) and CFX96 touch System (BioRad, USA).[18,19,53] The qPCR protocol is as follows: 95°C for 3 min followed by 40 cycles of 95°C for 10 s, 58°C for 10 s, 72°C for 30 s and final denaturation at 95°C for 10 s. As an internal control and to normalize the amount of template, tick beta actin or 5.8S rRNA amplicons were quantified. The standard curves were prepared using 10-fold serial dilutions starting from 1 to 0.000001 ng/μL of known quantities of respective gene fragments.

Tick cell line experiments with xanthurenic acid (XA)

Tick cells were incubated at 34°C. Tick cell line experiments with XA were performed.[18] Stock (10 mM) of XA (Sigma, USA) was made in 0.5 N NaOH solution.[18] A 1:10 dilution of the stock was prepared in 1× PBS to a final concentration of 1 mM and used for all experiments. Mock solution was prepared in a similar way but without XA. Tick cells (1×10^5) were seeded onto 12 well plates and incubated for 16–20 h. Following incubation, tick cells were treated with 100 μM concentration of XA for 4 h followed by *A. phagocytophilum* (isolated from 2×10^5 NCH-1 infected HL-60 cells) infection. Equal volumes of mock solution (corresponding to 100 μM volume) was added to control cells. The cells were then incubated for 48 h and processed further for RNA or DNA extractions and followed by qPCR to measure cell death marker gene transcripts or bacterial loads.

Tick cell line experiments with BIRB796, the p38 MAPK inhibitor

Stock (10 mM) of BIRB796 (Tocris, USA) was made in dimethyl sulfoxide (DMSO) solution. The stock solution was diluted with tick cell media to a final concentration of 10 μM. Mock solution was prepared in a similar

way but without BIRB796. Tick cells (1 × 10^5) were seeded onto 12 well plates and incubated for 16–20 h. Following incubation, tick cells were treated with 10 μM BIRB796 for 4 h followed by *A. phagocytophilum* (isolated from 2 × 10^5 NCH-1 infected HL-60 cells) infection. Equal volumes of mock solution (corresponding to 10 μM volume) was added to control cells. The cells were then incubated for 24 h and processed further for RNA and protein extractions to measure *p38 mapk* transcripts and protein levels, respectively. In other experiments, after 16–20 h post plating, tick cells were treated with 100 μM XA and 20 μM BIRB796 for 4 h followed by *A. phagocytophilum* infection. Equal volume of mock solutions (corresponding to 100 μM XA and 20 μM BIRB796 vol) were added to control cells. The cells were incubated for 24 h and processed for DNA extractions to measure bacterial loads.

Live/dead assay

The effects of XA on uninfected or *A. phagocytophilum*-infected tick cells were analyzed by using LIVE/DEAD Cell Imaging kit by following manufacturer's instructions.[19] Briefly, 2 × 10^5 tick cells were seeded in L15B300 medium on to 12 well plates and incubated for 24 h. After 24h, 100 μM XA was added to the cells followed by *A. phagocytophilum* infection. Cells were processed for live/dead staining on days 1, 3 and 6 post-infection and imaged at GFP channel and Texas Red channels with EVOS imaging system (Invitrogen/ThermoScientific Inc.). Different images were captured, and fluorescence intensity of dead cells was measured using TECAN spectrophotometer (TECAN, USA) at excitation/emission wavelength 570/602 nm. At least a minimum of five measurements were considered to calculate mean of fluorescence intensity. ImageJ (NIH) software was used to merge images taken in GFP and Texas Red channels from EVOS imaging system to generate overlay images shown in figures.

MTT assay

MTT [3-(4,5-dimethythiazol-2-yl)-2,5-diphenyl-2H-tetrazolium bromide] assay was used to measure the viability of *A. phagocytophilum*-infected tick cells after XA or 20 μM BIRB796 treatment.[54] Briefly, tick cells were plated at the density of 4 × 10^4 cells per well in a 96-well plate and incubated. After 16 h, 100 μM XA or 20 μM BIRB796 was added to the cells. After 4 h of treatment, cells were infected with *A. phagocytophilum* (isolated from 2 × 10^4 NCH-1-infected HL-60 cells). After 24 h post infection (p.i.), 20 μL ofold media was removed and 20 μL of MTT (5 mg/mL) stock solution was added to all wells. Plates were covered with aluminum foils and incubated at 37 °C for 4 h (until purple precipitate was visible). Following incubation, 100 μL of DMSO solvent was added and plates were further incubated at 37°C for another 15 min. Absorbance was read at 570 nm. Reference reads were taken at 690 nm. Absorbance values from 690 nm reference read were subtracted from the absorbance values obtained at 570 nm to determine the tick cell viability numbers.

Western blotting assay

Ten uninfected unfed nymphs and ten *A. phagocytophilum*-infected unfed nymphs were crushed and homogenized using pellet pestle cordless motor (Biospec, OK) and pellet pestle (VWR, USA) in modified-RIPA lysis buffer supplemented with EDTA-free protease inhibitor cocktail to generate tick lysates from uninfected or infected ticks, respectively. Mock or XA-treated tick cell lysates were prepared in modified-RIPA buffer supplemented with EDTA-free protease inhibitor cocktail. Tick cells (1 × 10^5) were seeded onto 12 well plates and incubated for 16–20 h. Following incubation, tick cells were treated with 100 μM of XA or 20 μM BIRB796 followed by *A. phagocytophilum* infection. Equal volumes of mock solution were added to control cells. The cells were then incubated for 24 h and then harvested to prepare total cell lysates in modified RIPA buffer supplemented with EDTA-free protease inhibitor cocktail. Protein concentrations were determined by Bradford (BCA) protein assay kit and as per manufacturer's recommendations. Tick or tick cells lysates (10–15 μg) were mixed with Laemmli sample buffer, boiled for 5 min and resolved on 12% reducing SDS-PAGE gels. Gels were run at 110 V. Gels were later stained with either Coomassie blue or transferred to nitrocellulose membranes. Coomassie-stained gel images served as loading controls. Membrane sections were blocked with 5% BSA in 1X TBST (1X TBS, 0.05% Tween 20). Primary antibody directed against PLD3, phospho- or total-p38 were used at a dilution of 1:500 in 5% BSA in 1X TBST. HRP-conjugated goat anti-rabbit secondary antibody was used at a dilution of 1:5,000 in 5% BSA in 1X TBST. Development of the chemiluminescent substrate was visualized using a BioRad ChemiDoc Touch Imaging System (BioRad, USA).

Endogenous XA measurement

Colorimetric assay was used to determine the endogenous XA.[40] Briefly, 8 mM solution of *N*, *N*-diethyl-*p*-phenylenediamine (DE-PPD) (ThermoScientific, USA), 300 IU/mL horseradish peroxidase (POD) (ThermoScientific, USA), XA or kynurenic acid (KA) (Sigma, USA) standards (2.5–150 μM), 0.1M acetate buffer (pH 4.3) were prepared with water. Unfed uninfected or *A. phagocytophilum*-infected nymphal ticks or tick cells were homogenized in water and supernatants were used as test samples. Infection was confirmed with qPCR using primers specific for *A. phagocytophilum*. For tick cell line experiments, 2×10^5 tick cells were seeded in L15B300 medium on to 12 well plates and incubated for 24 h. After incubation, one group of tick cells were infected with *A. phagocytophilum*, and other group was retained as uninfected controls. Tick cell samples were prepared after 48 h p.i. To 187.5 μL of 0.1M acetate buffer (pH 4.3), 46.8 μL DE-PPD, 46.8 μL of tick/tick cell samples or XA/KA standards, 9.37 μL POD, 9.37 μL of 30 mM hydrogen peroxide were added and mixed well. The mixture was allowed to stand at room temperature for 3 min. For blank solution, 9.37 μL water was used instead of hydrogen peroxide. Absorbance of the reaction mixtures was measured within 5 min at 750 nm.

Sequence alignment and analysis

GenBank accession numbers for the sequences used in the study are mentioned in Tables S1 and S2. Amino acid sequence alignments for PLD3, Syntaxin, SMP30, VPS26B and p38 MAPK orthologs from various organisms was performed using DNASTAR CLUSTALW alignment software. Sequence analyses were performed for *I. scapularis* PLD3, Syntaxin, SMP30, VPS26B and p38 MAPK with various organisms. The phylogenetic tree was constructed using the Neighbor-Joining method (BIONJ) using BIONJ algorithm in DNASTAR. The protein sequences for *I. scapularis* PLD3, Syntaxin, SMP30, VPS26B and p38 MAPK proteins were downloaded from GenBank and individually analyzed at PROSITE (http://prosite.expasy.org/) for the prediction of N-glycosylation, myristoylation, protein kinase C phosphorylation, casein kinase II phosphorylation and cAMP or c-GMP-dependent protein kinase phosphorylation sites.[55–57]

QUANTIFICATION AND STATISTICAL ANALYSIS

Statistical significance in the datasets was analyzed using GraphPad Prism6 software (https://www.graphpad.com/) and Microsoft Excel 2010 (https://www.microsoft.com). A Student's *t* test was used to compare statistical significance between the groups, or ANOVA was used to compare the group's variations. p values of <0.05 were considered significant in all analyses.